Gold Catalysis

How to cite:
International Edition: doi.org/10.1002/anie.202207518
German Edition: doi.org/10.1002/ange.202207518

Enantioselective Dearomative Cyclization Enabled by Asymmetric Cooperative Gold Catalysis

Ke Zhao, Philip Kohnke, Ziguang Yang, Xinpeng Cheng, Shu-Li You, and Liming Zhang**

Abstract: A gold(I)-catalyzed enantioselective dearomatization is achieved via metal-chiral ligand cooperation. A new and divergent synthesis of chiral bifunctional binaphthyl-2-ylphosphines is developed to allow rapid access to these ligands, which in turn facilitate the application of this chemistry to a broad substrate scope including 1-naphthols, 2-naphthols, and phenols. Enantiomeric excesses up to 98 % are achieved via selective acceleration of one enantiomer formation enabled by hydrogen bonding between substrate and ligand remote basic group. DFT calculations lend support to the cooperative catalysis and substantiate the reaction stereochemical outcomes.

Spirocarbocycles exist in a wide range of bioactive natural products[1] and provide comparatively rigid three-dimensional structural scaffolds for drug discovery.[1,2] Intramolecular catalytic asymmetric dearomatization (CADA)[3] offers a versatile and expedient strategy for the construction of chiral spirocarbocycles featuring a challenging quaternary carbon center. Recently, several types of chiral spirocycles have been constructed via asymmetric gold(I) catalysis[4] but the enantiomeric excesses are mostly moderate ($\leq$90 %) except when using parameterization to facilitate ligand optimization.[4g] Considering the versatility of gold catalysis in cyclization reactions,[5] there remain valuable yet unfulfilled opportunities to develop highly enantioselective construction of spirocarbocycles via gold-catalyzed dearomatization cyclizations.[6] In this work, we detail an advance in this area via asymmetric cooperative gold catalysis.[7] Due to the cooperation[8] between our rationally designed ligand and gold(I), the spirocyclization is accelerated enantioselectively, resulting in ee values up to 98 %, exhibiting a broad substrate scope including 1-naphthols and 2-naphthols and phenols, and permitting the formation of spirobicycles of different sizes and containing heteroatoms.

[*] K. Zhao, P. Kohnke, Z. Yang, X. Cheng, Prof. Dr. L. Zhang
Department of Chemistry and Biochemistry, University of California
Santa Barbara, CA 93106 (USA)
E-mail: zhang@chem.ucsb.edu
Homepage: https://zhang.chem.ucsb.edu/
Prof. Dr. S.-L. You
State Key Laboratory of Organometallic Chemistry, Shanghai Institute of Organic Chemistry, Chinese Academy of Sciences
345 Lingling Lu, Shanghai 200032 (China)
E-mail: slyou@sioc.ac.cn
Homepage: http://shuliyou.sioc.ac.cn/

We have recently developed several bifunctional biaryl-2-ylphosphine ligands of the general structure **L** featuring a remote basic group (Scheme 1A).[7] The interactions between the ligand basic group and substrate/nucleophile in bond-forming/breaking events achieve gold-ligand cooperation in catalysis. The catalytic reactions enabled/facilitated by these ligands either are not feasible when replaced by typical phosphine/N-heterocyclic carbene (NHC) ligands[9] or, in the case of WangPhos, experience substantial rate increases.[10] The latter acceleration phenomenon of the gold-ligand cooperation was harnessed in a gold-catalyzed enantioselective allenol cyclization by substantially accelerating the formation of one product enantiomer. As shown in Scheme 1B, with a chiral version of WangPhos featuring an axially chiral binaphthyl framework, i.e., (*R*)-**L1**, as the ligand, the reaction is nearly quantitative and exhibits >99 % ee with a catalyst loading of 100 ppm.[11] However, the application of this asymmetric acceleration phenomenon with substrates bearing a proprochiral C–C triple bond would necessitate stereoinduction at a distal prochiral center and hence be more challenging. We anticipated that the asymmetric dearomatization of phenols/naphthols en route

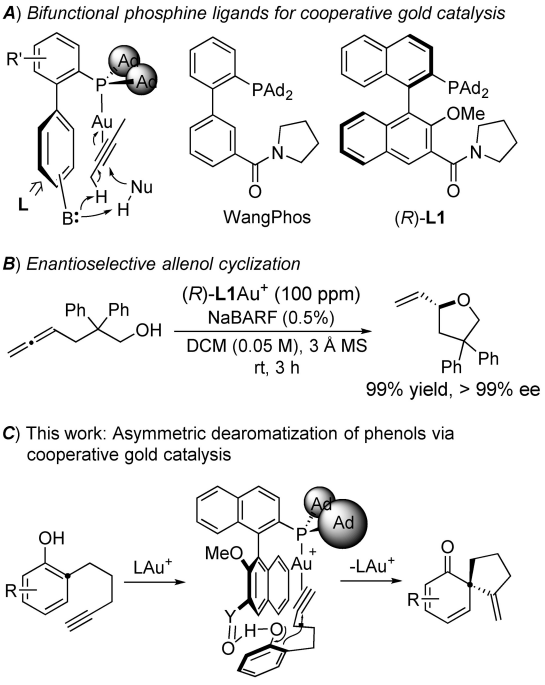

Scheme 1. Gold-ligand cooperation in catalysis and its implementation in intramolecular asymmetric dearomatization.

to chiral spirocyclic enone products, as outlined in Scheme 1C, might be an applicable system as the relevant intermolecular hydroarylation of terminal alkyne by 2-naphthol is accelerated by WangPhos.[10c]

We commenced our study by employing 1-(pent-4-yn-1-yl)naphthalen-2-ol (**5a**) as the substrate. As shown in Table 1, entry 1, the initial results by using our previously reported chiral amide-functionalized binaphthyl-2-ylphosphine ligand (*S*)-**L1** were encouraging, as the reaction is high-yielding and the enantiomeric excess of the spiroenone product **6a** was 74 %. Moreover, no product stemming from phenolic oxygen cyclization was detected.[12] Although the fast reaction—<10 min at ambient temperature—could readily permit the increase of the reaction enantioselectivity upon lowering the reaction temperature, we decided to first optimize the chiral bifunctional ligand by varying the essential basic group at the C3′ position of the binaphthyl skeleton.

Table 1: Conditions optimization.

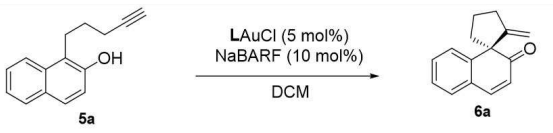

Entry	Ligand	Temp.	Time	Yield[a]	ee[b]
1	(S)-**L1**	rt	<10 min	99%	74%
2	(S)-**L2**	rt	<10 min	99%	75%
3	(S)-**L3**	rt	<10 min	98%	79%
4	(S)-**L4**	rt	<10 min	86%	90%
5	(S)-**4**	rt	45 min	76%	-48%
6	(S)-**L3**	-78 °C	6 h	86%	92%
7	(S)-**L4**	-78 °C	6 h	92%[c]	96%
8	JohnPhos	-78 °C	16 h	21%[d]	NA

[a] Determined by 1H NMR using diethyl phthalate as the internal standard. [b] Determined by chiral HPLC. [c] 84% isolated yield. [d] 24% conversion. NaBARF = sodium tetrakis[3,5-bis(trifluoromethyl)phenyl]borate; JohnPhos = (2-biphenylyl)di-tert-butylphosphine.

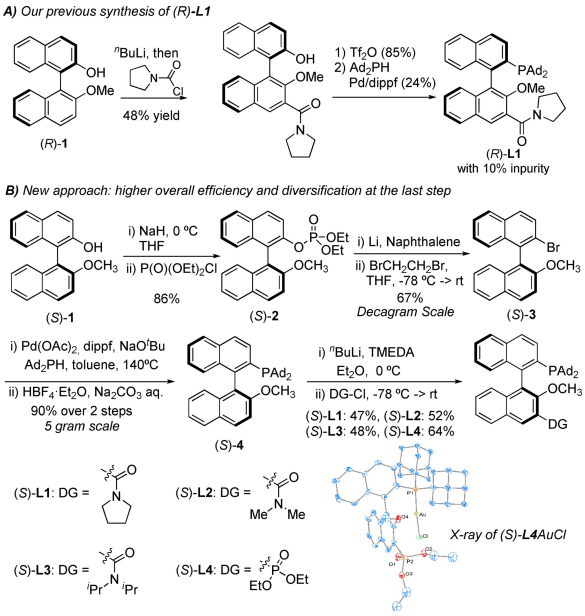

Scheme 2. Improved divergent ligand synthesis.

To this end, a ligand synthesis strategy conducive to late-stage diversification is highly desirable. However, our previous synthesis of (*R*)-**L1** (Scheme 2A), despite requiring only 3 steps from the monomethylated chiral BINOL (*R*)-**1**, installed the 1-pyrrolidinecarbonyl group at the beginning.[11] Moreover, the low overall yield – only 9.8 % - is mostly due to the low efficiency of installing the bulky PAd_2 group via a Pd-catalyzed cross-coupling between $HPAd_2$ and a binaphthyl triflate. The poor yield of this last step, i.e., 24 %, complicated product purification as (*R*)-**L1** was contaminated by 10 % impurity. To develop a divergent and more efficient ligand synthesis, we opted to install the PAd_2 group first and the remote basic group at the very end of the synthetic route. As shown in Scheme 2B, the binaphthyl-2-yl bromide (*S*)-**3** was prepared from (*S*)-**1** in a two-step sequence by following a related procedure.[13] Much to our delight, the Pd-catalyzed C–P coupling was remarkably efficient, affording the phosphine ligand (*S*)-**4** in 90 % yield. The last step of the ligand synthesis is to install different basic groups at the 3′ position via *ortho*-lithiation and electrophile trapping. The yield of this step was typically ≈50 %. Among the prepared ligands, (*S*)-**L1**, (*S*)-**L2**, and (*S*)-**L3** have different tertiary amide groups, while (*S*)-**L4** features a phosphonate moiety. The overall yields by following this 4-step route were ≥24 %, which in the case of (*S*)-**L1** is substantially better than that of our original approach. The structure of (*S*)-**L4** was confirmed by the X-ray diffraction study of its gold complex.[14]

With the additional ligands [i.e., (*S*)-**L2–L4**] in hand, we screened them against the dearomatization chemistry. As shown in Table 1, entries 2–4, under the same set of conditions, the *N*,*N*-diisopropylamide ligand (*S*)-**L3** and the phosphonate ligand (*S*)-**L4** performed noticeably better, with the latter offering the highest ee at room temperature. Remarkably, these reactions remained fast, proceeding to completion in <10 min. We also tried the reaction by using the unfunctionalized (*S*)-**4** as the ligand. As shown in entry 5, the reaction was notably slower and the enantiomeric excess (−48 % ee) is moderate and exhibits the opposite sense. This result confirms the key role of the remote basic group/directing group in dictating the stereochemical outcome and in accelerating the dearomatization. In the case of (*S*)-**L3**, as expected, the reaction ee was improved to 92 % when conducted at −78 °C (entry 6). Despite this low temperature, the accelerating nature of the catalysis permitted the completion of the reaction in just 6 hours. With the phosphonate (*S*)-**L4** as the ligand, the product ee was improved to 96 % ee at −78 °C (entry 7). By running the reaction at a preparative scale, **6a** was isolated in 84 % yield. The rate acceleration phenomenon by these bifunctional ligands is also evident by comparing with JohnPhos, a ligand of similar sterics and electronics to these bifunctional ligands but lacking the remote basic group as the reaction was substantially slow, reaching 21 % yield and 24 % conversion after 16 h at −78 °C (entry 8).

With the optimal conditions (Table 1, entry 7) in hand, the scope of the dearomatization of 1-(pent-4-ynyl)-2-naphthols was examined. As shown in Table 2A, a range of functional groups such as bromo, alkynyl, tertiary alcohol, Bpin, and NHBoc were readily accommodated on the non-phenolic benzene ring, and the enantioselectivity remained high in each case. In the cases of **6f** and **6g**, the amide ligand (*S*)-**L3** was preferred over (*S*)-**L4** for improved yields.

This cooperative catalysis also worked with 1-naphthols and induced mostly excellent enantiomeric excesses with the parent case (i.e., **6h**) and various substituted ones (i.e., **6i**–**6o**) (Table 2B). These reactions were generally slower than those of 2-naphthols and hence run at −40 °C or higher temperatures; moreover, (*S*)-**L3** was more effective than (*S*)-**L4**, offering higher yields and/or enantioselectivities. Various substituents such as methyl, vinyl, bromo, iodo, amide, and cyano groups were tolerated. Despite the raised temperatures, most of these reactions exhibited ≥97 % ee values, which are higher than those found with the 2-naphthol counterparts. The exception (87 % ee) in the case of the cyano product **6n** can be attributed to the comparative high reaction temperature (0 °C). The sluggishness of the reaction at lower temperatures is likely caused by the coordination of the cyano group to gold or the chloride scavenger Na^+ from NaBARF, although the electronic influence on the 1-naphthol reactivity could not be ruled out. The iodo product **6m** is crystalline and subjected to X-ray diffraction studies, which established the absolute configuration of the all-carbon quaternary center is *S*.[15] The configurations of all the other products are assigned by assuming that the (*S*)-ligands dictate the same arene ring facial selectivity. As a result, the products **6a**–**6g** formed from 2-naphthol substrates are assigned with the (*R*)-configuration.

To further expand the scope of naphthol substrates, we examined the substrates featuring O or NTs as part of the linker between the terminal alkyne and the naphthol ring. As shown in Table 2C, their reactions were again efficient and highly enantioselective, affording heterospirocyclic products **6p**, **6q**, and **6r** in ≥90 % ee and ≥95 % yields. In addition, this cooperative catalysis was applied to 6-*exo-dig* cyclizations. In comparison to the 5-*exo-dig* counterparts (i.e., **6a** and **6h**), the reactions forming the 6,6-spiroenone products **6s** and **6t**, respectively, were expectedly slower, and higher reaction temperatures were employed. As such, the enantiomeric excess of **6s** was a lower 88 %. Remarkably, 93 % ee was realized with **6t**, despite the reaction

Table 2: Reaction scope.[a]

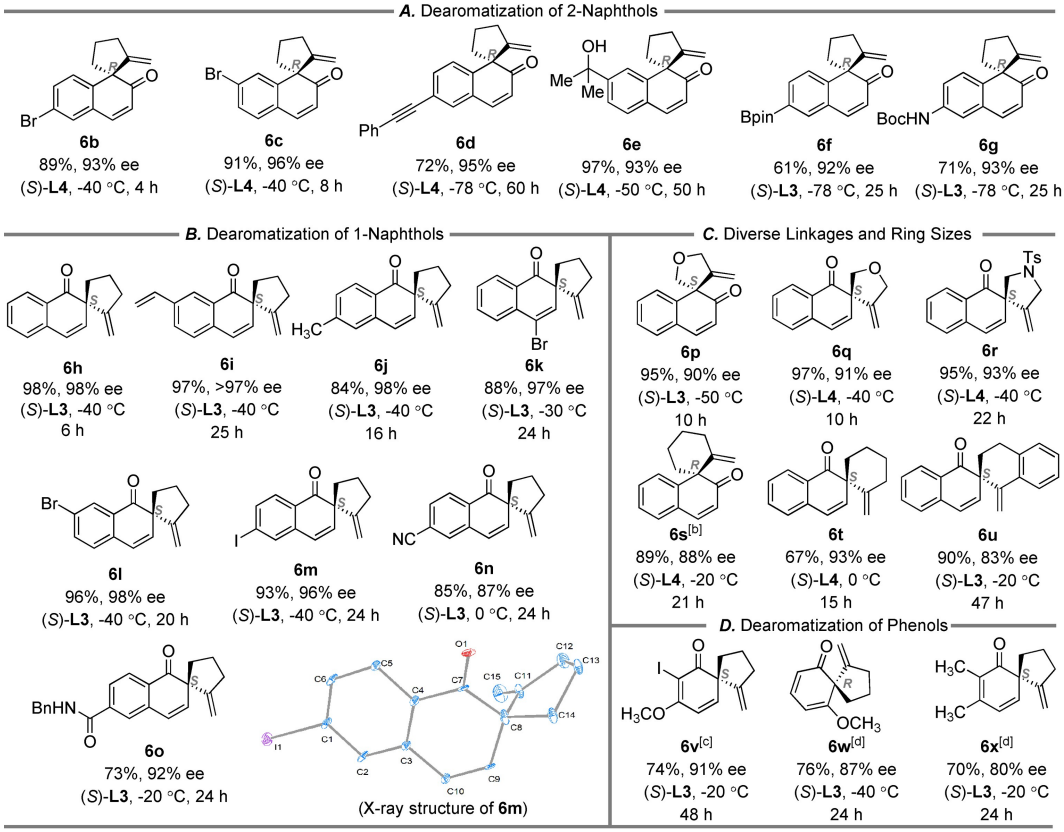

[a] Reaction run in DCM (0.1 M), the ligand and the reaction temperature indicated, isolated yield reported, and the ee values were determine by chiral HPLC analysis. [b] 5 Å molecular sieve is used as the drying reagent. [c] $PhCF_3$ is used as solvent. [d] Drierite is used as the drying reagent.

[a] Reaction run in DCM (0.1 M), the ligand and the reaction temperature indicated, isolated yield reported, and the ee values were determined by chiral HPLC analysis. [b] 5 Å molecular sieve is used as the drying reagent. [c] PhCF3 is used as solvent. [d] Drierite is used as the drying reagent.

temperature being 0 °C. With benzene fused to the linker, the ee of the product (**6u**) was 83 %.

Due to their higher aromatic stabilization energy, the dearomatization of phenols is more challenging than naphthols. To our delight, this cooperative strategy is also conducive to phenol dearomatization, and good to excellent enantioselectivities were realized (Table 2D). For example, the phenol substrate bearing a *meta*-methoxy and an *ortho*-iodo cyclized smoothly to afford the highly functionalized 5,6-spiroenone **6v** in moderate yield and with 91 % ee. The main side reaction is alkyne hydration. With the methoxy group substituted *ortho* to the alkyne-bearing alkyl group, the phenol was converted to the spiro product **6w** with 87 % ee at −40 °C. Both of these cases employed methoxy-substituted and hence electron-rich phenol substrates. However, the methoxy group could be replaced by weak electron-donating methyl groups, and the reaction still afforded the desired spirocyclic product **6x** with a decent 80 % ee.

Next we explored the synthetic utility of our method, which is showcased in Scheme 3. With the gold catalyst loading lowered to 0.5 mol% and the reaction temperature raised to 0 °C, the formation of **6l** remained highly enantioselective and efficient. This brominated product was subjected to the Suzuki coupling to afford the pyridine-functionalized **7** in 95 % yield, chemoselective ketone reduction by disiamylborane to deliver the alcohol **8** as the only diastereomer, and hydrogenation in the presence of Rh/C to afford the spiroketone **9** without affecting the bromo group.

To probe the cooperative nature of the catalysis and to understand asymmetric induction, we located the transition states of the enantio-determining cyclization step en route to the enantiomers of **6a** and **6h** (Figure 1) by performing DFT calculations. The reported Gibbs free energies were calculated under the experimental conditions with Truhlar's quasiharmonic approximation[16] using Goodvibes v3.[17] As shown in Figure 1A, the transition state **TS-R-6a** leading to (*R*)-**6a** is favored over **TS-S-6a** by 3.77 kcal mol^{-1} in free energy. This is consistent with the observed high enantioselectivity and supports the configuration assignment of the products **6a**–**6g**. The distances between the basic phosphonate oxygen (i.e., O1) and the phenolic hydrogen are an identical 1.63 Å for both **TS-S-6a** and **TS-R-6a**, revealing strong H bonding and supporting the cooperative participation of the ligand phosphonate functionality in the reaction. In addition, the lengths of the incipient C–C bond between C1 and C2, which are 2.23 Å and 2.22 Å for **TS-S-6a** and **TS-R-6a**, respectively, are nearly identical. The cause for the preference of **TS-R-6a**, however, can be attributed to the increased bending of the organogold moiety away from the pendant naphthyl ring in **TS-S-6a** to accommodate the requisite H-bonding during the cyclization. This bending is reflected by the difference of 10.4° in ∠P–Au–C3 and 1.8° in ∠C4–P–Au and by the substantially longer distances of C5–C3 and C5–Au in **TS-S-6a** than in **TS-R-6a**. The values of ∠C4–P–Au and ∠P–Au–Cl in the X-ray structure of (*S*)-**L4**AuCl[14] are 113.6° and 175.1°, respectively, which are closer to the related values of **TS-R-6a** than those of **TS-S-6a**. This is consistent with the increased bending in **TS-S-6a** being destabilizing. Similar differences are found between the transition states **TS-S-6h** and **TS-R-6h** (Figure 1B). **TS-S-6h** is favored by 4.23 kcal mol^{-1} in free energy, which is consistent with the highly enantioselective formation of (*S*)-**6h**. Of note, in both favored **TS-R-6a** and **TS-S-6h**, the same prochiral *Re* face is approached.

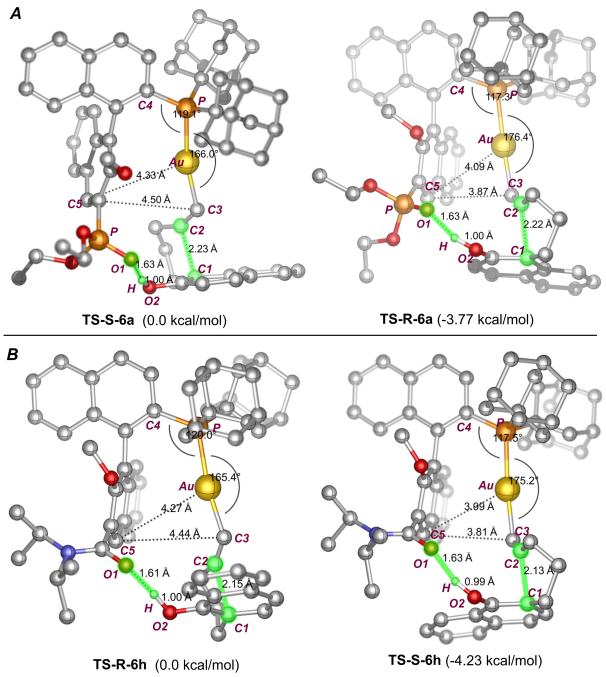

Figure 1. The cyclization transition states en route to **6a** and **6h** optimized by DFT at the M06/LANL2DZ (Au)-6-311G(d,p), SMD (DCM)//PBE0/LANL2DZ (Au)-6-311G(d,p)(P)-6-31G(d,p) (other atoms), SMD (DCM) level of theory. Relative Gibbs free energy shown.

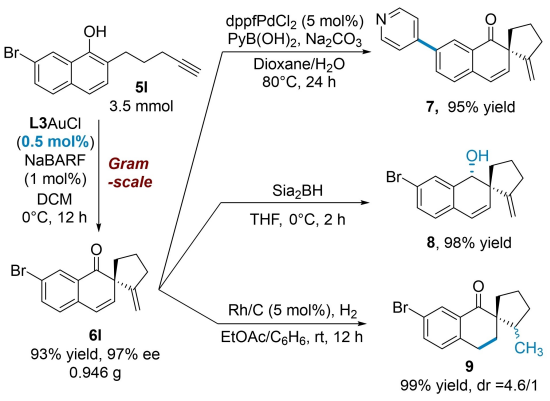

Scheme 3. Gram-scale reaction and synthetic applications.

In summary, we have developed a highly enantioselective dearomatization of naphthol and phenol derivatives. This asymmetric gold catalysis is enabled by chiral binaphthyl phosphine ligands featuring a remote amide or phosphonate substituent. A new and divergent synthesis of this class of bifunctional ligands is developed to facilitate their access.

DFT calculations support that the hydrogen bonding between substrate and the ligand basic group enables metal-ligand cooperation and accelerates enantioseletive cyclization. The products feature a spirocarbocyclic skeleton bearing a chiral all-carbon quaternary center and a synthetically versatile enone functionality. The reaction accommodates 1-naphthol, 2-naphthol, and phenol derivatives as substrates and exhibits enantioselectivities up to 98 % ee.

Acknowledgments

The authors thank NSF CHE 1800525 for financial support and NSF MRI-1920299 for the acquisition of Bruker 500 MHz and 400 MHz NMR instruments. The computational facilities are funded by the National Science Foundation (CNS-1725797) and administered by the Center for Scientific Computing (CSC), which is supported by the California NanoSystems Institute and the Materials Research Science and Engineering Center (MRSEC; NSF DMR 1720256) at UC Santa Barbara.

Conflict of Interest

The authors declare no conflict of interest.

Data Availability Statement

The data that support the findings of this study are available in the supplementary material of this article.

Keywords: Cyclization · Dearomatization · Enantioselectivity · Gold Catalysis · Metal-Ligand Cooperation

[1] L. K. Smith, I. R. Baxendale, *Org. Biomol. Chem.* **2015**, *13*, 9907–9933.

[2] a) Y. Zheng, C. M. Tice, S. B. Singh, *Bioorg. Med. Chem. Lett.* **2014**, *24*, 3673–3682; b) K. Hiesinger, D. Dar'in, E. Proschak, M. Krasavin, *J. Med. Chem.* **2021**, *64*, 150–183.

[3] a) C. Zheng, S.-L. You, *ACS Cent. Sci.* **2021**, *7*, 432–444; b) C. Zheng, S.-L. You, *Chem* **2016**, *1*, 830–857; c) Y. Q. Zhang, Y. B. Chen, J. R. Liu, S. Q. Wu, X. Y. Fan, Z. X. Zhang, X. Hong, L. W. Ye, *Nat. Chem.* **2021**, *13*, 1093–1100; d) M. Uyanik, T. Yasui, K. Ishihara, *Angew. Chem. Int. Ed.* **2010**, *49*, 2175–2177; *Angew. Chem.* **2010**, *122*, 2221–2223; e) M. Uyanik, T. Yasui, K. Ishihara, *Angew. Chem. Int. Ed.* **2013**, *52*, 9215–9218; *Angew. Chem.* **2013**, *125*, 9385–9388; f) M. Uyanik, K. Nishioka, R. Kondo, K. Ishihara, *Nat. Chem.* **2020**, *12*, 353–362.

[4] a) J. Oka, R. Okamoto, K. Noguchi, K. Tanaka, *Org. Lett.* **2015**, *17*, 676–679; b) N. Zheng, Y. Y. Chang, L. J. Zhang, J. X. Gong, Z. Yang, *Chem. Asian J.* **2016**, *11*, 371–375; c) J. An, A. Parodi, M. Monari, M. C. Reis, C. S. Lopez, M. Bandini, *Chem* **2017**, *23*, 17473–17477; d) J. M. Yang, P. H. Li, Y. Wei, X. Y. Tang, M. Shi, *Chem. Commun.* **2016**, *52*, 346–349; e) W. T. Wu, R. Q. Xu, L. Zhang, S. L. You, *Chem. Sci.* **2016**, *7*, 3427–3431; f) Y. Yu, Z. Zhang, A. Voituriez, N. Rabasso, G. Frison, A. Marinetti, X. Guinchard, *Chem. Commun.* **2021**, *57*, 10779–10782; g) Z. L. Niemeyer, S. Pindi, D. A. Khrakovsky, C. N. Kuzniewski, C. M. Hong, L. A. Joyce, M. S. Sigman, F. D. Toste, *J. Am. Chem. Soc.* **2017**, *139*, 12943–12946; h) A. Pradal, P. Y. Toullec, V. Michelet, *Synthesis* **2011**, 1501–1514; i) S. Sengupta, X. Shi, *ChemCatChem* **2010**, *2*, 609–619; j) V. Magné, A. Marinetti, V. Gandon, A. Voituriez, X. Guinchard, *Adv. Synth. Catal.* **2017**, *359*, 4036–4042.

[5] a) H. C. Shen, *Tetrahedron* **2008**, *64*, 7847–7870; b) B. Alcaide, P. Almendros, J. M. Alonso, *Molecules* **2011**, *16*, 7815–7843; c) W. Debrouwer, T. S. A. Heugebaert, B. I. Roman, C. V. Stevens, *Adv. Synth. Catal.* **2015**, *357*, 2975–3006; d) A. S. K. Hashmi, *Chem. Rev.* **2007**, *107*, 3180–3211; e) A. Fürstner, P. W. Davies, *Angew. Chem. Int. Ed.* **2007**, *46*, 3410–3449; *Angew. Chem.* **2007**, *119*, 3478–3519; f) S. M. Abu Sohel, R.-S. Liu, *Chem. Soc. Rev.* **2009**, *38*, 2269–2281; g) E. Jiménez-Núñez, A. M. Echavarren, *Chem. Rev.* **2008**, *108*, 3326–3350.

[6] a) W.-T. Wu, L. Zhang, S.-L. You, *Acta Chim. Sin.* **2017**, *75*, 419–438; b) L. Ding, W.-T. Wu, L. Zhang, S.-L. You, *Org. Lett.* **2020**, *22*, 5861–5865; c) M. D. Aparece, P. A. Vadola, *Org. Lett.* **2014**, *16*, 6008–6011; d) T. Nemoto, N. Matsuo, Y. Hamada, *Adv. Synth. Catal.* **2014**, *356*, 2417–2421; e) H. Wang, K. Wang, Y. Xiang, H. Jiang, X. Wan, N. Li, B. Tang, *Adv. Synth. Catal.* **2018**, *360*, 2352–2357.

[7] X. Cheng, L. Zhang, *CCS Chem.* **2021**, *3*, 1989–2002.

[8] a) H. Grützmacher, *Angew. Chem. Int. Ed.* **2008**, *47*, 1814–1818; *Angew. Chem.* **2008**, *120*, 1838–1842; b) J. R. Khusnutdinova, D. Milstein, *Angew. Chem. Int. Ed.* **2015**, *54*, 12236–12273; *Angew. Chem.* **2015**, *127*, 12406–12445.

[9] a) Z. Wang, Y. Wang, L. Zhang, *J. Am. Chem. Soc.* **2014**, *136*, 8887–8890; b) Z. Wang, A. Ying, Z. Fan, C. Hervieu, L. Zhang, *ACS Catal.* **2017**, *7*, 3676–3680; c) X. Li, X. Ma, Z. Wang, P.-N. Liu, L. Zhang, *Angew. Chem. Int. Ed.* **2019**, *58*, 17180–17184; *Angew. Chem.* **2019**, *131*, 17340–17344; d) T. Li, L. Zhang, *J. Am. Chem. Soc.* **2018**, *140*, 17439–17443.

[10] a) Y. Wang, Z. Wang, Y. Li, G. Wu, Z. Cao, L. Zhang, *Nat. Commun.* **2014**, *5*, 3470; b) X. Li, S. Liao, Z. Wang, L. Zhang, *Org. Lett.* **2017**, *19*, 3687–3690; c) T. Li, Y. Yang, B. Luo, B. Li, L. Zong, W. Kong, H. Yang, X. Cheng, L. Zhang, *Org. Lett.* **2020**, *22*, 6045–6049.

[11] Z. Wang, C. Nicolini, C. Hervieu, Y. F. Wong, G. Zanoni, L. Zhang, *J. Am. Chem. Soc.* **2017**, *139*, 16064–16067.

[12] C. Zheng, L. Wang, J. Li, L. Wang, D. Z. Wang, *Org. Lett.* **2013**, *15*, 4046–4049.

[13] C. Kim, T. Uchida, T. Katsuki, *Chem. Commun.* **2012**, *48*, 7188–7190.

[14] Deposition number 2149502 (for **L4**AuCl) contains the supplementary crystallographic data for this paper. These data are provided free of charge by the joint Cambridge Crystallographic Data Centre and Fachinformationszentrum Karlsruhe Access Structures service.

[15] Deposition number 2149501 (for **6m**) contains the supplementary crystallographic data for this paper. These data are provided free of charge by the joint Cambridge Crystallographic Data Centre and Fachinformationszentrum Karlsruhe Access Structures service.

[16] R. F. Ribeiro, A. V. Marenich, C. J. Cramer, D. G. Truhlar, *J. Phys. Chem. B* **2011**, *115*, 14556–14562.

[17] G. Luchini, J. V. Alegre-Requena, I. Funes-Ardoiz, R. S. Paton, *F1000Research* **2020**, *9*, 291.

Manuscript received: May 22, 2022
Accepted manuscript online: July 17, 2022
Version of record online: ■■, ■■

Communications

Gold Catalysis

K. Zhao, P. Kohnke, Z. Yang, X. Cheng, S.-L. You,* L. Zhang* **e202207518**

Enantioselective Dearomative Cyclization Enabled by Asymmetric Cooperative Gold Catalysis

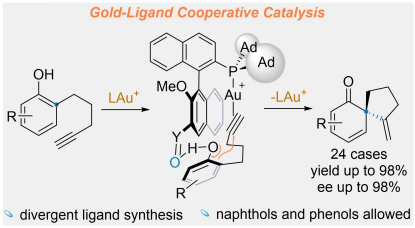

Gold-ligand cooperation permits catalytic enantioselective dearomatization of 1-naphthols, 2-naphthols, and phenols. This work is facilitated by the development of a divergent synthesis of chiral bifunctional binaphthyl-2-ylphosphine ligands. Enantiomeric excesses up to 98% are realized. DFT calculations lend support to the cooperative nature of the catalysis and the observed stereochemical outcome.